# Interface dynamics during Cu shadow-mask physical vapor deposition on nonmetallic substrates

P. C. dos Santos Claro, P. L. Schilardi, B. Blum, M. F. Castez, and R. C. Salvarezza*

*Instituto de Investigaciones Fisicoquímicas Teóricas y Aplicadas (INIFTA), Facultad de Ciencias Exactas, Universidad Nacional de La Plata-CONICET, Sucursal 4 Casilla de Correo 16, B1904DPI La Plata, Argentina*

(Received 10 August 2007; published 26 November 2007)

We have studied the interface dynamics during the growth of microscopic ordered Cu features deposited on different nonmetallic substrates by shadow-mask physical vapor deposition. Optical and atomic force microscopy data show the formation of either transparent or opaque patterned Cu depending on the film thickness. The evolution of the patterned film, the shadowed and the exposed regions, and the pattern shape are well described in terms of a continuous mesoscopic model, implying that masked deposition induces (through evaporation-condensation processes) an overall downhill current that results, under the small slope approximation, in Edwards-Wilkinson behavior.

DOI: 10.1103/PhysRevB.76.205436 PACS number(s): 68.03.Hj, 68.03.Fg, 68.37.−d, 81.15.Aa

## INTRODUCTION

Thin films are usually deposited on surfaces using techniques based on atomic or molecular physics and chemistry. Physical vapor deposition (PVD) of thin films relies on the removal of atoms from a solid or a liquid by energetic means and the subsequent deposition of these atoms on a nearby surface, following ballistic trajectories.[1] Frequently, masks either on or just above the surfaces are used to select deposition areas for building complex architectures with different physical properties. Evaporation through masks either in well defined proximity or in contact with the surface, allows depositing a controlled amount of material at the locations where it is needed, thereby avoiding further processing. In contrast, surface patterning with lithographic processes requires the use of resist spinning and chemical solvents for the development of exposed areas.[2] These steps cannot be applied to surfaces functionalized with organic molecules or biomolecules. This makes shadow-mask techniques promising for patterning unconventional materials on unconventional surfaces without photolithography, and therefore eliminating chemical contamination as well as mechanical damage of the substrates.[2] Given these characteristics, the fields that particularly benefit from shadow-mask techniques include biochemical microsystems, MEMS, and molecular electronic devices.

At early deposition stages, continuous metallic films that are sufficiently thin compared to the wavelength of light can be optically transparent. The thickness of a film at the point where the transmitted light amplitude is reduced to about half of the incident light is referred to as its "skin depth."[3] Partial transparency tends to be seen in films that are thick compared to their skin depth. Metal films that are optically transparent are important for applications of functionalized surfaces in biology because experiments often require observation of cells or microorganisms on the substrates by transmission optical microscopy.[4]

The combined use of these properties with shadow mask PVD allows the development of transparent or opaque patterned metallic films that have applications in a number of fields of research and technology. However, the control of the precise location and amount of the depositing material by shadow-mask PVD requires a delicate balance between different physical processes such as direct incorporation of arriving particles, remitted flux, evaporation-condensation, shadowing, lateral growth, and surface diffusion.[5] In fact, physical properties and structure of thin films depend crucially on deposition kinetics. It is therefore important to gain further insight into the role played by each of these physical processes on the growth kinetics and final shape of the films.

Continuous models have been proposed to describe the evolution of growth fronts during deposition.[6] It is generally accepted that surface diffusion and step-edge energy barriers determine the interface dynamics at the nanoscale while the physical contributions acting at the microscale are more elusive. In this range it is expected that lateral growth and evaporation-condensation influence markedly the surface topography.[6] In the latter case the Edwards Wilkinson (EW) equation[7] should account for the growth front evolution although only a few experimental systems have been reported to be described by this continuous model.[8] Besides, it is expected that continuous models are valid in the asymptotic limit although in practice it is the transient response of the interface that is relevant for device fabrication. It has been shown that the shape evolution of micropatterned substrates has been useful to test the validity of different continuous models during early stages of deposition.[9]

Here, we use AFM and optical microscopy to investigate the growth of transparent-opaque patterned Cu films by shadow-mask physical vapor deposition on dodecanethiol-coated Au, polycyanoacrilate, and glass substrates. We find that the evolution of the micropatterned film, shadowed and exposed areas, and pattern shape are well described by considering that masked deposition induces evaporation-condensation processes that lead to an overall downhill current that produces, for interfaces under the small slope approximation, an Edwards-Wilkinson behavior.

## EXPERIMENTAL

The experimental setup is shown in Fig. 1. Polycyanoacrilate, glass, or dodecanethiol-covered Au substrates (prepared by 2 h immersion in 50 $\mu$M dodecanethiol containing ethanolic solution) were used. Hexagonal Ni meshes (bar

 ©2007 The American Physical Society

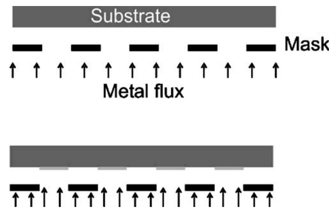


FIG. 1. Scheme showing the experimental setup used in micropattern preparation. The metallic Cu flux is masked by a hexagonal Ni grid close to the sample (1 mm from the sample).

width: 8 $\mu$m, hole width: 29 $\mu$m, thickness: 40 $\mu$m) were used as masks to produce the Cu patterns. These masks result in micropatterns suitable to be analyzed by atomic force microscopy at different places and free of tip-sample artifacts. The base pressure in the evaporation chamber ranged from $2.5\times10^{-7}$ torr to $3\times10^{-7}$ torr and the separation between the metal evaporation source and the substrate surface was 20 cm so that the incoming flux was nearly perpendicular to the substrate. The deposition time ($t$) was varied from 25 seconds to 540 seconds with the substrate at room temperature.

Optical microscopy and atomic force microscopy (AFM, Digital Instruments Santa Barbara, CA) operating in the contact mode were used to characterize the Cu films. $Si_3N_4$ tips were used for the AFM measurements.

## RESULTS AND DISCUSSION

Figures 2(a) and 2(b) shows images taken with an optical microscope for (a) masked polycyanoacrilate and (b) glass substrates, after exposure to Cu vapor for a deposition time $t<100$ s. The films show transparent regions (bright outlines) separating the opaque hexagons. Conductivity measurements show that the film is continuous, implying that the bright regions are covered by a transparent Cu film.

For $t>100$ s we cannot obtain images with the optical microscope, indicating that a continuous opaque Cu film is present. This is clear evidence that for longer deposition times the growth at shadowed regions becomes important.

The evolution of the growth fronts of the exposed and shadowed regions can be investigated over a broader range of deposition times with AFM techniques. Typical AFM images of the patterned Cu films on the different substrates are shown in Figs. 3(a) and 3(b) (240 s$<t<$360 s). Well defined Cu hexagonal features are present irrespective of the substrate utilized. In this case, the bright regions correspond to exposed regions while the dark interhexagons regions correspond to the shadowed ones. The interface dynamics of the films at both the shadowed and exposed regions was followed through the time evolution of the root mean square roughness ($w$) at the hexagon tops ($w_e$, bright regions in Figs. 3) and at the interhexagons areas ($w_s$, dark regions in Figs. 3). In both cases, $w$ was measured from $7\times7$ $\mu m^2$ AFM images, i.e., the maximum size of the shadowed regions for a proper comparison of roughness data. We observe that after an initial increase, $w_e$ and $w_s$ rapidly saturate reaching a relatively small value $\approx$10–20 nm in the range 40 s$<t<$300 s. We also observe that $w_e$ and $w_s$ follow a similar trend irrespective of the sample region (and substrate) indicating that the deposition mechanism is the same although the local deposition rates are very different.

We now concentrate on the evolution of the overall system. The contour level plots built from AFM images provide experimental information about the hexagon shape evolution as a function of deposition time. While the size of the hexagon at half height is preserved ($\approx$29 $\mu$m), the hexagon tops become narrower with time and develop a parabolic shape (Fig. 4). On the other hand, the hexagon-base widths increase with deposition time, finally covering completely the masked regions. The advance into and thickening of the masked regions are responsible for the transparent-opaque transition observed in the system.

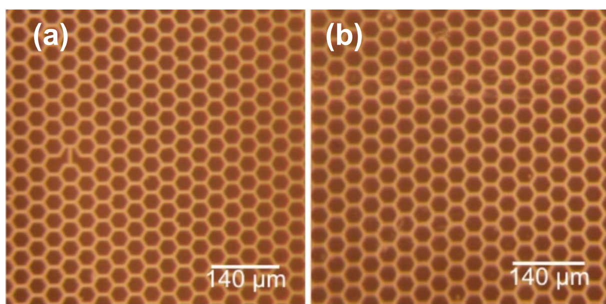


FIG. 2. (Color online) Transmission optical microscope images of transparent-opaque Cu films on (a) polycyanoacrilate and (b) glass. Deposition time=60 s.

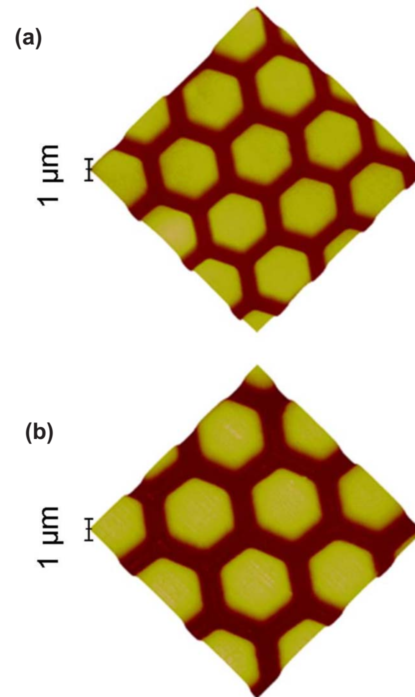


FIG. 3. (Color online) 3D AFM images of opaque patterned Cu films on different substrates for different deposition times. (a) $123\times123$ $\mu m^2$, substrate: polycyanoacrilate, $t=240$ s and (b) $100\times100$ $\mu m^2$, substrate: thiol-covered Au, $t=360$ s.

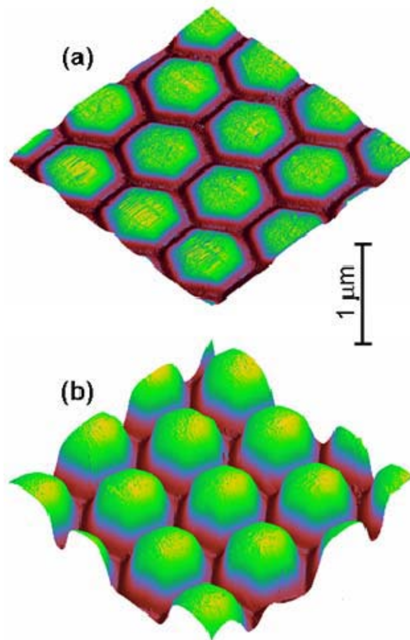


FIG. 4. (Color online) 3D AFM-image contour-level plots ($95\times95\ \mu m^2$) of Cu micropatterns for different growth times: (a) 60 s and (b) 540 s. (a) Evidences the advance of Cu from the exposed regions (green) to the masked regions (black). (b) Shows rounded tops of the hexagons (green-yellow).

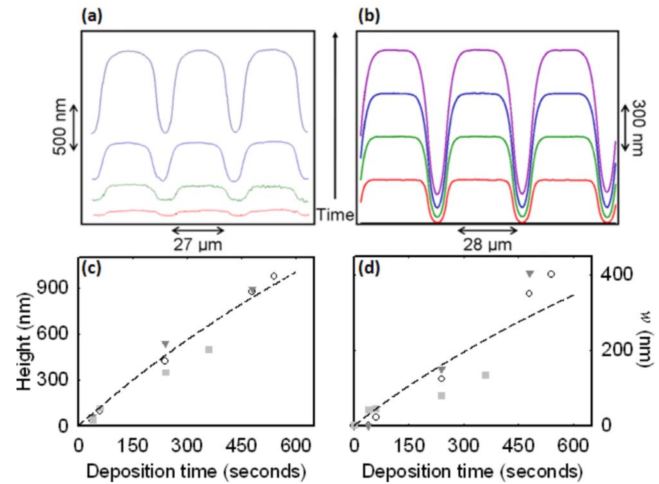


FIG. 5. (Color online) (a) AFM profiles showing the evolution of the growth front for Cu films on glass. $t=40$, 60, 240, 540 s. (b) Profiles showing the evolution of the growth front calculated from Eq. (1), $t=150$, 300, 450, 600 s. Parameters in the model were $F=2\ \mathrm{nm\,s^{-1}}$, $\nu=1.5\times10^4\ \mathrm{nm^2\,s^{-1}}$ and the temperature was 350 K. (c) Maximum height (hexagon top-valley vertical distance measured from the profiles) vs $t$ for Cu films grown on the different substrates (○) glass, (▼) polycyanoacrylate, (■) dodecanethiol-covered Au. Dashed line: maximum height (hexagon top-valley vertical distance) vs $t$ plot calculated from Eq. (1) and $F=2\ \mathrm{nm\,s^{-1}}$, temperature$=350$ K, $\nu=1.5\times10^4\ \mathrm{nm^2\,s^{-1}}$. (d) $w$ vs $t$ plot for Cu films grown on the different substrates (○) glass, (▼) polycyanoacrylate, (■) dodecanethiol-covered Au. Dashed line: $w$ vs $t$ plot calculated from Eq. (1) and $F=2\ \mathrm{nm\,s^{-1}}$, temperature$=350$ K, $\nu=1.5\times10^4\ \mathrm{nm^2\,s^{-1}}$.

The cross sections in Fig. 5(a) show the shape evolution of the hexagonal features as a function of deposition time. The increase in the height ($h$) of the hexagons is nearly linear with $t$ [Fig. 5(c)], irrespective of the substrate. The slope of these plots corresponds to $\Delta v$, the difference in the growth velocity between the exposed and shadowed regions of the substrates. The $\Delta v$ value derived from these plots is $\approx1\ \mathrm{nm\,s^{-1}}$. A similar linear dependence was found for the $w$ vs $t$ plot [Fig. 5(d)]. This means that the growth front evolves according to $w\propto t^{\beta}$ with $\beta\approx1$.[5] The value of $\beta$ indicates an unstable interface resulting from the different deposition rates at exposed and shadowed regions. The difference in growth velocity results in the faster increase in height of the hexagonal features, i.e., the interface width increases continuously with deposition time, at least for the time range studied.

A model that describes our experimental system at initial stages of deposition should account for the following experimental facts:

(1) The shadowed regions receive a non-null overall flow of material leading to a transparent-opaque transition. The interface evolution at exposed and shadowed regions is similar despite the difference in growth rate.

(2) The hexagon tops decrease in size with deposition time.

(3) The hexagon bases increase in size with deposition time.

(4) The difference in growth velocity and surface roughness (the overall amplitude of the growth front) between the exposed and shadowed region are nearly linear with time.

We have performed computer simulations on a continuous mesoscopic $1+1$-dimensional model for the growth of solid films on microstructured substrates. For this task, we have employed a modified version of a model recently introduced by some of us[10,12,13] for the study of pattern preserving phenomena and pattern decay from surface diffusion currents. For details on the original model the reader can see Refs. 10–13. For now we only discuss the general aspects of the model and the changes introduced in it to adjust to the particular physical situation in our current experiments. The interface is parametrized by a vectorial function $\mathbf{r}(s,t)$, where $s$ is the arc length parameter and $t$ is time. Evolution proceeds following the local outward normal in a Huygens's construction fashion. To include the mask in the model, we assume that a directed flow of particles impacts over the interface and, for normal incidence, leads to a non-null local growth rate on exposed parts of the interface, while in shadowed parts of the interface we have a null flow. Surface diffusion currents are present in the model and have been taken as proportional to the local curvature gradient.[14–16] As evaporation-condensation processes are expected to be important in our system (the proposed physical origin for such processes are discussed below in this section), we have introduced a term in the main model's equation proportional to the local curvature $C$, since it is a well established fact that evaporation-condensation processes lead to the emergence of curvature-dependent terms in the underlying coarse-grained continuous description.[12,14,15,17]

We can summarize the physical content of the model by writing the deterministic part of the local growth rate $v_n$, which reads

$$v_n = F\cos(\gamma)M(s) + \nu C - K\partial^2 C/\partial s^2, \quad (1)$$

where $F$ is the deposition rate, $\gamma$ is the angle between the local normal of the interface and the incidence direction[13,18] and $M(s)$ is a function that is equal to 1 for exposed regions and equal to zero for shadowed ones. The value of the coefficient $K$ depends strongly on temperature, and we have taken the dependence reported in Ref. 19 for Cu substrates. The value of the coefficient $\nu$ was fitted with the experimental results presented in this paper. It is important to notice that the term $\nu C$ becomes the leading one in front of the surface diffusion term $K\partial^2 C/\partial s^2$ at the length scales and temperature ranges considered in this paper. In fact, simulations performed including only surface diffusion currents, with no evaporation-condensation term, have become far from the experimental pattern evolution in the microscale. This means that surface diffusion as the unique relaxation process is not enough to explain what is observed. Figure 5(b) shows several profiles during interface evolution in the model. The similarity with experimental profiles [Fig. 5(a)] becomes evident. Note, that in contrast to the experimental profiles shown in Fig. 5(a), the calculated profiles are referred to the substrate level. Also $h$ (calculated as the difference between the pattern tops and the valleys), and $w$ vs $t$ plots calculated with the model and those observed experimentally [Figs. 5(c) and 5(d)] are in good agreement, thus we can say that masked flow and evaporation-condensation are the most relevant shape-determining processes in our system. Additionally, the patterns generated in our growth process have aspect ratios consistent with the small-slopes approximation, thus the curvature $C$ can be replaced with the familiar Laplacian term from the Edwards-Wilkinson equation.[7] In this sense, the main relaxation process in our system adopts an Edwards-Wilkinson-type behavior.

Now we discuss the origin of the Laplacian term in Eq. (1). We consider that the emergence of relevant evaporation-condensation flows in our physical system is due to thermal gradients generated among exposed (hot) regions and shadowed (cold) regions.[20] In fact, those parts of the interface exposed to the incident beam receive not only an incoming mass flow but also they receive an incoming energy flow. This energy flow increases the local temperature on the exposed regions, promoting, in this way, an overall evaporation flow over such regions. Moreover, individual collisions between particles in the incident beam against particles on the interface can help "the pumping" of surface atoms to the vapor phase, increasing the evaporation rate above the equilibrium thermal value. Particles emitted by exposed regions can become condensed over other places on the interface, coming back into the solid phase. This condensation process takes place preferably at cold regions of the interface, i.e., at those shadowed regions that cannot receive mass and energy from the incident beam. We have further experimental evidence for the existence of a vaporlike phase in our system, since we have observed Cu deposition on the nickel mask face opposed to the incident beam. This experimental evidence supports our interpretation because it is proof that a non-negligible amount of Cu in a vaporlike phase is present above the interface.

Finally, a comment should be made about the insignificant influence of the substrate on the interface dynamics. We know that for the dodecanethiol-covered Au substrate the initial stage of Cu deposition is different because Cu atoms diffuse through defects present at the self-assembled monolayer (domain boundaries, molecular vacancies), and then form nuclei that grow inside the defects.[21–23] These nuclei emerge from the monolayer and finally overlap to form a continuous Cu deposit. Our results show that these initial processes (diffusion, nucleation, and growth) that take place inside the organic layer, i.e., at the nanoscale, since the dodecanethiol thickness is 1.7 nm, do not affect the later stages of growth of the Cu deposit at the micrometer scale.

## CONCLUSIONS

We have grown Cu micropatterns on rigid polymer, organic film-coated Au, and glass substrates by shadow-mask physical vapor deposition. The substrate does not influence the growth process of the Cu deposit. The deposition process results in the fast growth of ordered features at the exposed regions at a high rate, and a slower growth at shadowed regions. We have studied a $1+1$-dimensional model trying to improve our understanding of experimental results. The interface evolution in simulations compares well with the evolution in the real system. Simulations with a masked flow have described correctly the measured shape evolution, even in quantitative aspects like roughness and overall height at the early stages of deposition. The only relevant relaxation process in the model is the evaporation-condensation contribution that, in the small slopes approximation, leads to an Edwards-Wilkinson[5,7] Laplacian term in the evolution equation.

It is important to note that our model not only reproduces global experimental interface evolution properties such as roughness and scaling exponents, but also describes correctly the point-to-point interface dynamics. In fact, as was discussed in Ref. 9, several surface growth models often employed in the literature correctly account for scaling properties of experimental systems but, nevertheless, they fail to reproduce the whole interface shape evolution observed in real experiments.

## ACKNOWLEDGMENTS

We are grateful to ANPCyT (PICT 02-11111, PICT 03-17492, PAE 22771), UNLP (Project No. 11/X425), and CONICET (PIP 6075, PIP 5248) for financial support of this work.

*Corresponding author. FAX: 54-221-4254642; robsalva@inifta.unlp.edu.ar

[1] S. M. Rossnagel, J. Vac. Sci. Technol. A **21**, S74 (2003).
[2] G. Kim, B. Kim, and J. Brugger, Sens. Actuators, A **A107**, 132 (2003).
[3] M. Fox, *Optical Properties of Solids* (Oxford University Press, New York, 2002).
[4] J. C. Love, L. A. Estroff, J. K. Kriebel, R. G. Nuzzo, and G. M. Whitesides, Chem. Rev. (Washington, D.C.) **105**, 1103 (2005).
[5] A. L. Barabási and H. E. Stanley, *Fractal Concepts in Surface Growth* (Cambridge University Press, Cambridge, England, 1995).
[6] J. Villain, J. Phys. I **1**, 19 (1991); M. Kardar, G. Parisi, and Y.-C. Zhang, Phys. Rev. Lett. **56**, 889 (1986); Z.-W. Lai and S. Das Sarma, *ibid.* **66**, 2348 (1991); T. Sun, H. Guo, and M. Grant, Phys. Rev. A **40**, 6763 (1989).
[7] S. F. Edwards and D. R. Wilkinson, Proc. R. Soc. London, Ser. A **381**, 17 (1982).
[8] L. Vázquez, R. C. Salvarezza, and A. J. Arvia, Phys. Rev. Lett. **79**, 709 (1997).
[9] H.-C. Kan, S. Shah, T. Tadyyon-Eslami, and R. J. Phaneuf, Phys. Rev. Lett. **92**, 146101 (2004).
[10] M. F. Castez, M. H. Fonticelli, O. Azzaroni, R. C. Salvarezza, and H. G. Solari, Appl. Phys. Lett. **87**, 123104 (2005).
[11] W. W. Mullins, J. Appl. Phys. **28**, 333 (1957).
[12] M. F. Castez and E. V. Albano, J. Phys. Chem. C **111**, 4606 (2007).
[13] M. F. Castez, R. C. Salvarezza, and H. G. Solari, Phys. Rev. E **73**, 011607 (2006).
[14] W. W. Mullins, J. Appl. Phys. **30**, 77 (1959).
[15] C. Herring, in *Physics of Powder Metallurgy*, edited by W. E. Kingston (McGraw-Hill Book Co. Inc., New York, 1951), Chap. 8.
[16] J. Lapujoulade, Surf. Sci. Rep. **20**, 191 (1994).
[17] Y. P. Zhao, G. C. Wang, and T. M. Lu, Phys. Rev. B **58**, 13909 (1998).
[18] G. S. Bales and A. Zangwill, Phys. Rev. Lett. **63**, 692 (1989).
[19] G. Andreasen, P. L. Schilardi, O. Azzaroni, and R. C. Salvarezza, Langmuir **18**, 10430 (2002).
[20] V. Deepak and A. Gaur, Semicond. Sci. Technol. **16**, 665 (2001).
[21] P. L. Schilardi, P. Dip, P. C. dos Santos Claro, G. A. Benítez, M. H. Fonticelli, O. Azzaroni, and R. C. Salvarezza, Chem.-Eur. J. **12**, 38 (2006).
[22] I. Thom, G. Hähner, and M. Buck, Appl. Phys. Lett. **87**, 024101 (2005).
[23] Y. Tai, A. Shaporenko, H. Noda, M. Grunze, and M. Zharnikov, Adv. Mater. (Weinheim, Ger.) **17**, 1745 (2005).